Available online at www.sciencedirect.com
ScienceDirect
Journal of Solid State Chemistry 181 (2008) 1213–1219
JOURNAL OF SOLID STATE CHEMISTRY
www.elsevier.com/locate/jssc

Synthesis and characterization of a new layered organic–inorganic hybrid nickel(II) 1,4:5,8-naphthalenediimide *bis*-phosphonate, exhibiting canted antiferromagnetism, with $T_c \sim 21$ K

Elvira M. Bauer[a,*], Carlo Bellitto[a], Carlos J. Gómez García[b,*], Guido Righini[a]

[a]*Istituto di Struttura della Materia del CNR, Sez. di Montelibretti, Via Salaria km 29.3, I-00016 Monterotondo Stazione, Italy*
[b]*Instituto de Ciencia Molecular, University of Valencia, Pol La Coma s/n, E-46980 Paterna, Valencia, Spain*

Received 13 November 2007; received in revised form 31 January 2008; accepted 17 February 2008
Available online 4 March 2008

Abstract

A new Ni(II) layered hybrid organic-inorganic compound of formula $Ni_2[(NDI\text{-}BP)(H_2O)_2]\cdot 2H_2O$ has been prepared in very mild conditions from *N*,*N*′-*bis*(2-phosphonoethyl)napthalene-1,4:5,8-tetracarboximide (NDI-BP ligand) and $NiCl_2$. The X-ray powder structure characterization of the title compound suggests a pillared layered organic-inorganic hybrid structure. The distance between the organic and inorganic layers has been found to be 17.8 Å. The inorganic layers consist of corner sharing $[NiO_5(H_2O)]$ octahedra and they are pillared by the diphosphonate groups. DC and AC magnetic measurements as a function of temperature and field indicate the presence of 2D antiferromagnetic exchange interactions between the nearest-neighbor Ni(II) ions below 100 K. A long-range magnetic ordering at $T_c \sim 21$ K has been established and is attributed to the presence of spin canting. AC magnetic measurements as a function of temperature at different frequencies confirm the occurrence of the magnetic ordering temperature at $T = 21$ K and the presence of a slight structural disorder in the title compound.

Keywords: Ni(II) naphthalenediimidephosphonate; Hybrid organic–inorganic compound; Magnetic measurements; Canted antiferromagnet

1. Introduction

The design and preparation of new organic–inorganic hybrid compounds are receiving a great attention today since they can provide interesting examples of multifunctional materials [1]. The chemical assembly of an inorganic component with an organic one has in fact the potential to provide more than one useful (physical and/or chemical) property in the same lattice, in which each subnetwork exhibits its own properties. This class of compounds includes several types of functional hybrids and is found in intercalation compounds, donor–acceptor compounds, coordination complexes, etc. Of remarkable interest is the class of organic conductors which are basically organic/inorganic solids formed by stacks of organic π-electron donor molecules and several types of inorganic anions containing magnetic ions, such as the paramagnetic $[M(ox)_3]^{3-}$ anions (M = Fe(III), Cr(III); ox = oxalate dianion) or the polymeric ferromagnetic anion $[Mn(II)Cr(III)(ox)_3]_n^{n-}$. The chemical self-assembling of these moieties combines electrical and magnetic properties and has provided the largest family of paramagnetic metals [2–4], the first example of paramagnetic superconductor [5] and the first ferromagnetic metal [6]. With the aim of obtaining new examples of multifunctional hybrids we have carried out their preparation by chemical reaction of a complex ligand, containing both the functional and donor groups, with paramagnetic transition metal ions. For this purpose the following molecular building blocks were chosen: (a) the functional RPO_3H_2 ligand, R = organic group and (b) transition metal ions with unpaired spins. The reason for this can be found in the fact that recently several interesting magnetic divalent

*Corresponding authors. Fax: +39 06 90672316 (E.M. Bauer), +34 96 3543273 (C.J. Gómez García).
E-mail addresses: Elvira.Bauer@ism.cnr.it (E.M. Bauer), carlos.gomez@uv.es (C.J. Gómez García).

0022-4596/$ - see front matter © 2008 Elsevier Inc. All rights reserved.
doi:10.1016/j.jssc.2008.02.014

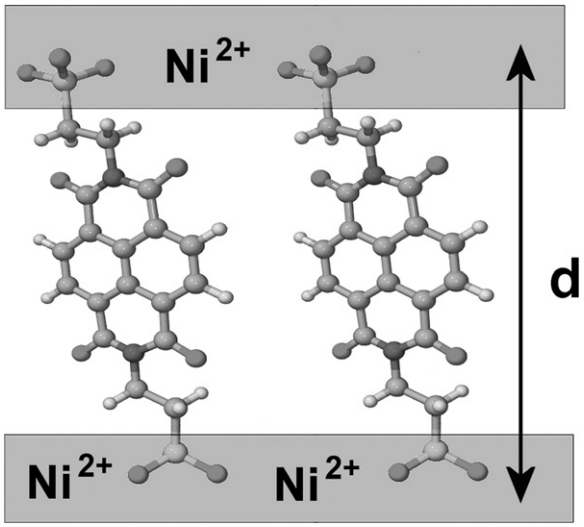

Scheme 1. The *N,N′-bis*(2-phosphonoethyl)napthalene-1,4:5,8-tetracarboximide (NDI-BP) ligand.

metal phosphonates have been prepared and characterized [7–14], and that the *R*-group can be chemically modified. An interesting functional molecule as an *R*-group is represented by the 1,4:5,8-naphthalenediimide molecule (NDI) hereafter [15,16]. This aromatic molecule, in fact, features interesting photochemical and electrochemical properties and can be functionalized with two donor groups such as the phosphonic groups (see Scheme 1) [17]. The chemical insertion of these pendent donor groups makes the ligand ideal for self-assembling hybrid compounds.

Here we report on the synthesis, the structural and magnetic characterization of a new functional magnetic hybrid organic–inorganic Ni(II) *bis*-phosphonate, $Ni_2[(NDI\text{-}BP)(H_2O)_2]\cdot 2H_2O$.

2. Experimental

2.1. Materials and methods

Naphthalene-1,4:5,8-tetracarboxylic anhydride, aminoethylphosphonic acid, $NH_2(CH_2)_2PO_3H_2$ (Aldrich Chemical Co.), Ni(II) chloride hexahydrate, $NiCl_2\cdot 6H_2O$ and urea (Carlo ERBA) were of analytical grade and were used without further purification. *N,N′*-dimethylformamide was purified before use by distillation over molecular sieves and under inert atmosphere. HPLC water was used as solvent.

2.2. Synthesis of N,N′-bis(2-phosphonoethyl)napthalene-1,4:5,8-tetracarboximide (NDI-BP)

The synthesis of the ligand NDI-BP has been carried out by following a previously reported procedure [17]. The yellow product was purified twice by dissolving it in a NaOH solution and precipitated by the exposure to vapors of HCl. The final product was washed with cooled water and with water/ethanol, pure ethanol and finally was dried under vacuum. Anal. Calcd. (%) for $C_{18}H_{16}N_2O_{10}P_2$: C, 44.80; H, 3.34; N, 5.81; Found: C, 42.45; H, 3.78; N, 5.46.

2.3. Synthesis of $Ni_2[(NDI\text{-}BP)(H_2O)_2]\cdot 2H_2O$

The title compound has been prepared by mixing the *bis*-phosphonate ligand with $NiCl_2$ and urea in water in a Ni:NDI-BP:urea molar ratio of 2:1:4. The resulting mixture was refluxed for 7 days. A beige powdered solid precipitated, which was filtered off, washed with water, acetone and air-dried. Anal. Calcd. (%) for $C_{18}H_{20}N_2O_{14}P_2Ni_2$: C, 32.38; H, 3.02; N, 4.19; P, 9.28; Ni, 17.58. Found: C, 32.40; H, 3.01; N, 4.72; P, 8.63; Ni, 17.94.

2.4. Characterization and physical measurements

Elemental analyses have been performed by the "Servizio di Microanalisi della Area di Ricerca di Roma del CNR", and by Malissa & Reuter, Lindlar, Germany. Thermogravimetric (TGA) data were obtained in flowing dry nitrogen at a heating rate of 10°/min on a Stanton-Redcroft STA-781 thermoanalyzer. The FT-IR absorption spectra were recorded on a Perkin Elmer 621 spectrophotometer using KBr pellets. The UV-visible reflectance spectra of the samples were recorded on a Varian Cary 5 spectrophotometer. Variable temperature susceptibility measurements were carried out in the temperature range 2–300 K with an applied magnetic field of 0.1 T on a freshly prepared powdered sample ($m = 18.44$ mg), with a Quantum Design MPMS-XL-5 SQUID magnetometer. Isothermal magnetizations and hysteresis cycles were measured for the same sample at different temperatures in the −5 to 5 T range. AC susceptibility measurements were performed on the same sample with an oscillating magnetic field of 0.395 mT in the frequency range 1–1000 Hz. The susceptibility data were corrected for the sample holder (a sealed plastic bag of 8.39 mg), previously measured using the same conditions and for the diamagnetic contribution of the salt as deduced by using Pascal's constant tables ($\chi_{dia} = -291.4\times10^{-6}$ emu K mol^{-1}). In order to confirm the reproducibility of the magnetic measurements, we performed a second series of magnetic measurements with an older sample in a different SQUID susceptometer that gave, within experimental errors, identical results.

2.5. X-ray data collection

Room temperature X-ray powder diffraction data were recorded on a Seifert XRD-3000 diffractometer, Bragg-Brentano geometry, equipped with a curved graphite monochromator [$\lambda(CuK\alpha_{1,2}) = 1.54056/1.5444$ Å] and a scintillation detector. The data were collected with a step size of 0.02°, $\Delta 2\theta$ and at count time of 8 s per step over the range $3° < 2\theta < 80°$. The diffractometer zero point was determined from an external Si standard.

3. Results and discussion

The layered NDI-containing Ni(II) *bis*-phosphonate $Ni_2[(NDI\text{-}BP)(H_2O)_2]\cdot 2H_2O$ was prepared by a mixture of the ligand NDI-BP and $NiCl_2$ in water and by refluxing the solution in presence of urea for a few days. The compound was isolated from the solution as a beige poorly crystalline powder and characterized by elemental analyses, TGA (DSC) and XRPD techniques as well as by the UV-visible and FT-IR absorption spectroscopy. The TGA of $Ni_2[(NDI\text{-}BP)(H_2O)_2]\cdot 2H_2O$ shows several stepwise mass losses (see Fig. S1). Below 100 °C a loss of ~6% is due to water of crystallization (~2 molecules). Above 100 °C the compound starts to lose coordinated water and it stops at ~266 °C. The total observed weight loss at this stage is ~10.7%, a value which corresponds to four water molecules per formula unit (the calculated weight loss for four water molecule per formula unit is 10.8%). These results indicate that two water molecules per formula unit are coordinated to the nickel atoms. Above 270 °C the compound loses mass in two steps: the first one from 270 to ~310 °C and the second one up to 475 °C. The total weight loss is 6.23% probably due to the imide bond cleavage of the NDI-BP ligand, which generates hydrocarbon molecules like CH_4 or higher ones.

3.1. X-ray powder structural characterization

The X-ray diffraction pattern of the hybrid compound $Ni_2[(NDI\text{-}BP)(H_2O)_2]\cdot 2H_2O$ is reported in Fig. 1 and exhibits essentially in the low 2θ-angle region ($0k0$) reflections characteristic of a lamellar structure with low interplanar correlations. A similar pattern has been observed in the layered long-chain $Ni[(O_3P(CH_2)_{17}CH_3)(H_2O)]$ compound [18]. The pattern has been used to estimate the interlayer spacing. From the experimental *d*-spacing values an interlayer distance of 17.8 Å is found. If the NDI-BP molecules were perpendicular to the plane of the inorganic layer in the lattice, the expected interlayer distance would be ca. 18 Å, as calculated by summing the thickness of the inorganic layer (i.e. ~3.2 Å as has been estimated from the crystal structure of $Ni[(O_3PCH_3)(H_2O)]$ [18] and ~14.8 Å, the lengths of the NDI-BP organic group measured between the P atoms). This result suggests therefore that the ligands are pillared and nearly perpendicular with respect to the $[NiO_6]$ inorganic layers (see inset in Fig. 1). Some additional insights of the molecular structure are obtained from absorption spectroscopy and thermal studies (see below).

3.2. Optical properties

The IR absorption spectra of $Ni_2[(NDI\text{-}BP)(H_2O)_2]\cdot 2H_2O$ and of the pure NDI-BP are reported in Fig. 2. The most interesting feature is found in the pure ligand, where two intense and broad bands centered at 2758 and 2276 cm^{-1} and assignable to OH stretching vibration of the POH groups are observed. These bands disappear when the Ni complex is formed, thus suggesting that the ligand is completely deprotonated in the compound. Another important characteristic feature is the presence in the Ni-derivative of strong H–O–H stretching vibrations of the coordinated water molecule at 3479 and 3358 cm^{-1}. The strong and sharp nature of these bands indicates that the water molecules are coordinated to the metal ions in this compound. These results are in agreement with TGA studies, from which two coordinated water molecules per formula unit were identified. The medium band, observed at 1658 cm^{-1}, is assigned to the H_2O bending frequency. Three strong bands are observed in the range 1200–970 cm^{-1} and are assigned to symmetric (1000 and 978 cm^{-1}) and asymmetric (1096 cm^{-1}) $[PO_3]^{2-}$ group stretching. The reflectance spectra of the free ligand and of the Ni(II) complex were recorded in the visible and in the near infrared regions (see Fig. S2). The metal complex displays three main bands: the first one, very broad, shows a maximum centered at ~1400 nm ($^3A_{2g}\rightarrow{}^3T_{2g}(F)$), the second band, in the visible, a peak centered at ~794 nm ($^3A_{2g}\rightarrow{}^3T_{1g}(F)$) and a spin allowed transition at ~400 nm

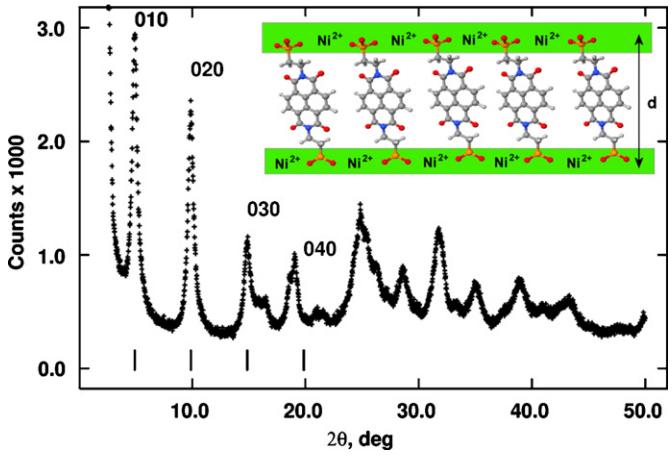

Fig. 1. Powder-X-ray diffraction pattern of $Ni_2[(NDI\text{-}BP)(H_2O)_2]\cdot 2H_2O$. A schematic structural model is given in the inset.

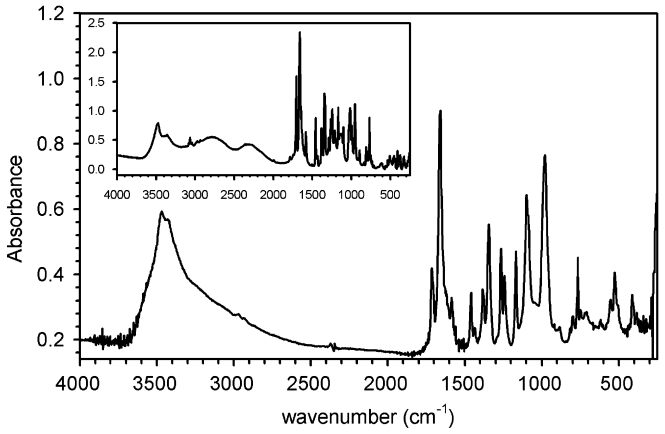

Fig. 2. Absorption FTIR spectrum of $Ni_2[(NDI\text{-}BP)(H_2O)_2]\cdot 2H_2O$ in the KBr region. The IR spectrum of the ligand is given in the inset.

($^3A_{2g} \rightarrow {}^3T_{1g}(P)$). The spin forbidden electronic transition is located at ~708 nm ($^3A_{2g} \rightarrow {}^1E_g$) [19]. This optical spectrum is similar to those observed previously in $Ni_2[(O_3PC_6H_4–O–C_6H_4PO_3)(H_2O)_2]$ [20] and in $NH_4NiPO_4 \cdot H_2O$ [21] where the Ni(II) ions are coordinated in distorted octahedron by ligand oxygens and one water molecule. Moreover, in the optical spectrum of the free ligand and in that of the title complex, two additional peaks at 510 and 360 nm are observed. The band at 510 nm can be tentatively assigned to the *inter*-molecular electronic transition of π-stacked molecular aggregates, while that at 360 nm to the *intra*-molecular $\pi \rightarrow \pi^*$ transition of the ligand [22,23].

3.3. Magnetic properties

Fig. 3 shows the thermal variation of the product of the molar magnetic susceptibility per Ni dimer (χ_m) times the temperature ($\chi_m T$) of the title compound. The room temperature $\chi_m T$ value of ca. 2.3 emu K mol^{-1} corresponds to the expected value for two non interacting high-spin Ni(II) ions (d^8, $S = 1$) per formula unit [24]. As the temperature is lowered, the $\chi_m T$ value decreases until a minimum of ca. 2.18 emu K mol^{-1} is reached at T~80 K and then increases again (see inset in Fig. 3). This behavior is indicative of antiferromagnetic exchange interactions between the Ni(II) ions. The antiferromagnetic exchange interactions can also be observed in the Curie–Weiss plot (χ_m^{-1} vs. T, not shown) which is linear above 80 K with a Curie constant, C, of 1.19 emu K mol^{-1} per Ni(II) ion (corresponding to a g-value of 2.18) and a negative Weiss temperature, θ, of −19 K. Below ca. 80 K the $\chi_m T$ value increases abruptly and reaches a maximum at T~20 K (see Fig. 3). This increase is also featured in the χ_m vs. T plot (not shown) and suggests the appearing of a long-range magnetic ordering at temperatures below T~20 K. In order to confirm the antiferromagnetic nature of the exchange interactions and the two dimensional character of the magnetic network, the magnetic data above the minimum were fitted according to the quadratic-layer antiferromagnet model of M.E. Lines for an $S = 1$ spin system [25]. This model reproduces satisfactorily the experimental data in the 300–90 K temperature range (solid line in the inset of Fig. 3), with a g-value of 2.135(1) and an exchange parameter $J = -1.20(3)$ cm^{-1} (considering the Hamiltonian as $H = -JS_iS_j$). These results confirm: (a) the antiferromagnetic nature of the magnetic coupling between the Ni(II) ions and (b) the two dimensional character of the magnetic lattice. Although we do not have the full crystal structure, we can conclude that the intralayer Ni–O–Ni angles must be far from 90° since the Ni–O–Ni coupling is ferromagnetic when this angle is in the range of 90 ± 14° [26,27]. In fact, in a very similar layered Ni diphosphonate compound Ni–O–Ni angles in the range of 120–125° were found [28]. Since the magnetic network is only formed by octahedral Ni(II) ions, bridged by oxygen atoms of the phosphonic ligands, and because the magnetic coupling between the metal ions is antiferromagnetic, the long-range ordering must be attributed to the presence of a spin canting between the $S = 1$ spin ground states of the Ni(II) ions (i.e. a not complete alignment of the spins up and down that leads to a not complete cancellation of their magnetic moments).

An additional proof of the presence of long-range ordering comes from the zero field and field cooled magnetizations: thus, below ca. ~20 K the magnetic susceptibility of the title compound shows a different behavior when it is cooled in zero field (ZFC) or in the presence of a magnetic field (FC) (see Fig. 4). If the sample is cooled down to 2 K in zero field a very low signal appears as a consequence of the absence of a preferential orientation of the magnetic domains in the weak ferromagnet. When warming the sample in the presence of a DC magnetic field of 10 mT, the susceptibility increases due to

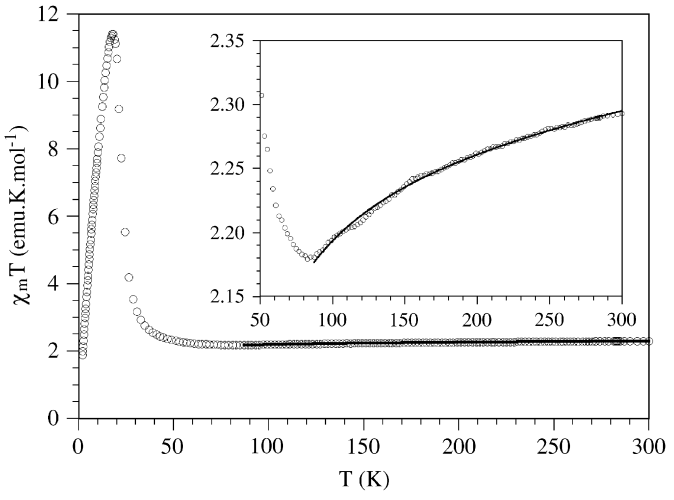

Fig. 3. Thermal variation of $\chi_m T$ in the temperature range 2–300 K. Inset: plot of $\chi_m T$ vs. T in the 30–300 K range. Solid line is the best fit to the model (see text).

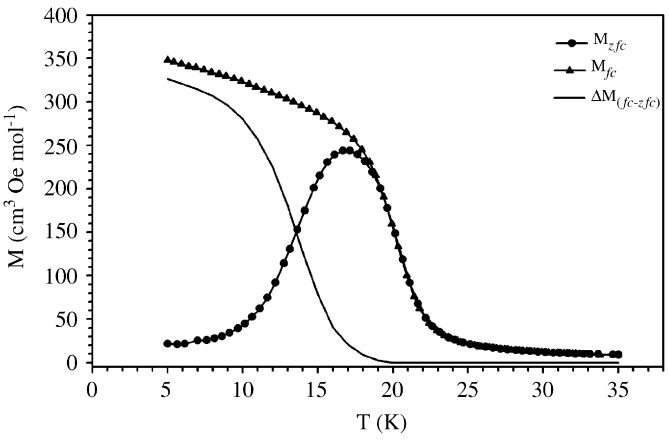

Fig. 4. Plots of zero field cooled (ZFC, black circles) and field cooled (FC, black triangles) magnetic susceptibilities vs. temperature measured at 0.1 T. The difference of the plots is the irreversible magnetization (solid line).

the progressive orientation of the domains and reaches a broad maximum centered at ca. 19 K. Above this temperature the magnetic susceptibility is typical of a paramagnet. The field cooled susceptibility curve diverges from the ZFC one below ca. 20 K due to the formation of magnetic domains aligned with the applied DC field. The difference between the FC and ZFC plots represents the irreversible magnetization and decreases as the temperature increases and becomes almost zero at the ordering temperature of ca. 20 K (Fig. 4).

In order to get more information about the long-range magnetic ordered state and the ordering temperature, T_c, AC susceptibility measurements in the temperature range 2–30 K at different AC frequencies in the 1–1000 Hz range have been performed (see Fig. 5). As expected for a weak ferromagnet, the AC measurements show the presence of a peak in both, the in-phase χ' and the out-of-phase χ'' components of the AC susceptibility. These measurements indicate that the ordering temperature, T_c, is 21.0 K (the temperature at which χ'' becomes non-zero, see inset in Fig. 5). A close inspection of the peaks in both, χ' and χ'' plots reveals a slight peak shift towards lower temperatures as the frequency of the oscillating field decreases. This frequency dependence is usually observed in superparamagnetic systems, spin glasses, spin-like glasses and in disordered materials [29]. However, these peak shifts are very small in the title compound. Thus, the relative shift of the AC peaks ($\Delta T_f/T_f$) per decade of frequencies ($\Delta T_f/(T_f \log(\nu))$ is only 0.013 for the χ' peak. This value is too small compared with those usually found in superparamagnets (which are about 20 times bigger) and is in the normal range found for spin-like glass systems (which are in the 0.004–0.018 range) [29]. A further evidence of the spin glass like behavior of the ordered phase comes from the fit of the frequency shift of the χ' peak to an Arrhenius law ($\ln(\nu) = \ln(\nu_0) - E_a/kT$), that gives unphysical values of $\nu_0 = 1080$ Hz and $E_a = 3430$ K, typical of spin-glass like systems) and to the Vogel–Fülcher law ($\nu = \nu_0 \exp[-E_a/k_B(T_f - T_0)]$), that provides much more realistic parameters: $E_a/k_B = 1.0(4)$ K, $\nu_0 = 4.5\,10^8$ Hz and $T_0 = 18.4(1)$ K, all in the normal range observed for spin glass-like materials) [29]. Therefore, we can conclude that a slight (probably occupational) disorder exists in the title compound which accounts for the slight frequency shift of the χ' and χ'' peaks. Probably this disorder may also contribute to the low crystallinity observed in the title compound. A very similar frequency shift has already been observed in other two- and three-dimensional magnets containing bimetallic networks of the type $[Fe^{III}M^{II}(C_2O_4)_3]^-$ (M^{II} = Mn, Fe, Co and Ni) and attributed to the presence of a positional disorder on the Fe(III) and Fe(II) ions in the case of the $[Fe^{III}Fe^{II}(C_2O_4)_3]^-$ complex [30–32].

A further evidence of the weak ferromagnetic behavior of the title compound comes from the field dependence of the magnetization (0–5 T) and the hysteresis loops recorded at different temperatures. As can be seen in Fig. 6, the title compound presents hysteresis loops for temperatures below 20 K with coercive fields of 252.5, 145.7, 39.0, 3.3 and 2.3 mT at 2, 5, 10, 15 and 20 K, respectively (inset in Fig. 6). The isothermal magnetization vs. field plot shows a continuous increase with increasing magnetic field, as a result of a progressive alignment of the Ni(II) spins. The fact that the magnetization plots do not show any saturation, even at the highest measured field (5 T), together with the low magnetization values at 5 T (below 1 μ_B in all cases, see Fig. 6) confirms that the title compound behaves as a weak ferromagnet.

In order to determine the canting angle of the local $S = 1$ spin states, we have estimated the saturation magnetization (M_R) by extrapolation at $H = 0$ of the linear part of M vs. H plots at different measured temperatures (see inset in Fig. 6). This extrapolation leads to saturation values of ca. 0.12–0.13 μ_B in the temperature range 2–15 K and a slightly lower value of 0.10 μ_B at 20 K. This is probably due to the

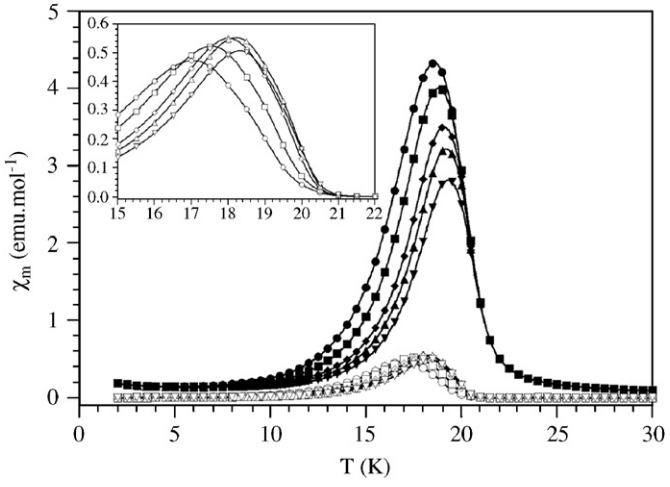

Fig. 5. AC magnetic measurements (χ' filled symbols, χ'' empty symbols) of the title compound at 1 Hz (circles), 10 Hz (squares), 110 Hz (rhombs), 332 Hz (up-triangles) and 997 Hz (down triangles).

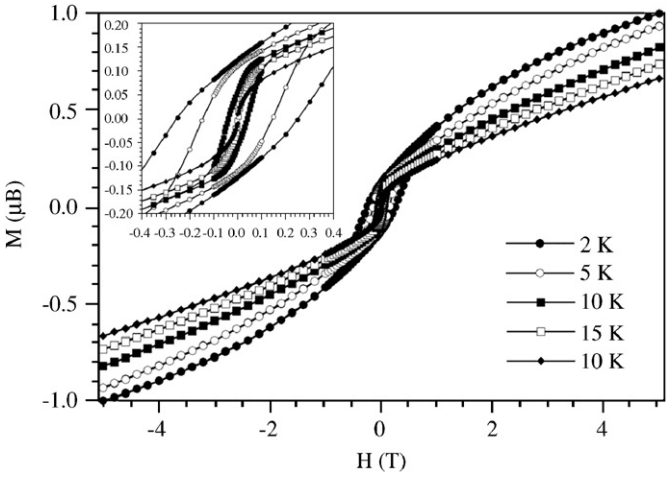

Fig. 6. Hysteresis loops ($M/N\beta$ vs. H) of the title compound at 2, 5, 10, 15 and 20 K. Inset: zoom of the plots in the field range 0 ± 0.4 T.

fact that at this temperature the magnetic transition is not complete and the correlation length, therefore, is not very high. These saturation values are about 3% of the expected values for a ferromagnetic alignment of the two $S=1$ spins per formula unit ($M_S = 2\,g\,S \approx 4.4\,\mu_B$), indicating that the canting angle, α, in the title compound is ca. 1.6–1.7° ($\sin\alpha = M_R/M_S$).

Time-dependent measurements at low temperature show a relaxation process that cannot be reproduced with a typical exponential decay model ($M(t) = M_0 \exp[(-t/\tau)^{1-n}]$). Furthermore, the Cole–Cole plot does not show the typical semicircular shape expected for a single relaxation process. These facts may be attributed to the presence of different spin domains with different environments as a consequence of the local positional disorder in the Ni layer.

The magnetic behavior showed by the title compound has been previously observed in the layered hybrid $Ni[(C_{18}H_{37}PO_3)(H_2O)]$, $T_c = 20\,K$ [18]. Surprisingly, the establishment of weak ferromagnetism is not always observed in Ni(II) organophosphonates. Thus, although weak ferromagnetism has been recently observed in two $Ni[(RPO_3)(H_2O)]$ compounds ($R = C_3H_7$, $T_c = 16\,K$, $R = C_6H_5$, $T_c = 5\,K$), other Ni(II) organophosphonates as $Ni_2[(O_3P(C_6H_4)PO_3)(H_2O)_2]$ [33] and $Ni_2[(O_3P(CH_2)_2PO_3)(H_2O)_2]$ [28] are antiferromagnets with a Neél temperature below $T = 13\,K$ in the latter case. This is in contrast with what has been observed in the series $Fe[(C_nH_{2n+1}PO_3)(H_2O)]$ [34], and in $Mn[(C_nH_{2n+1}PO_3)(H_2O)]$ [35,36], $n=1$, 2…, where the transition temperatures have been found to be nearly independent from the interlayer distance in the hybrid. Work is in progress to elucidate this point.

4. Conclusions

A new hybrid organic–inorganic Ni(II) diphosphonate containing 1,4:5,8-naphthalenediimide moiety of formula $Ni_2[(NDI\text{-}BP)(H_2O)_2]\cdot 2H_2O$ has been prepared by reaction of $NiCl_2$ and the diphosphonate ligand in water in the molar ratio Ni:NDI-BP = 2:1. The reaction affords a poor crystalline powder, which has prevented determination of the crystal structure. However, the low-angle region XRPD pattern, characterized by the presence of ($0k0$) reflections, suggests a layered pillared structure for the title compound and a crystal structure, probably similar to that observed in metal *bis*-phosphonates $M_2[(O_3PC_6H_4PO_3)(H_2O)]$, M = Co(II), Ni(II) [33]. The inorganic layer is formed by high-spin octahedral $[NiO_5(H_2O)]$ chromophores, as inferred from optical and magnetic findings. An indirect information on the lamellar structure of the title compound is given by the $\chi_m T$ vs. T plot in the high temperature region, which fits according to the quadratic-layer AF model proposed by M.E. Lines. The magnetic data show antiferromagnetic exchange interactions between the Ni(II) ions and revealed the presence of a spontaneous magnetization below $T = 21\,K$ arising from a spin canting. The weak-ferromagnet presents coercive fields as high as 252.5 mT at 2 K.

Acknowledgments

This work is supported by MIUR FIRB 2001 program, the Consiglio Nazionale delle Ricerche (Italy), the European Union (MAGMANet network of excellence and COST Action D35-WG-0011-05) and the Spanish Ministerio de Educación y Ciencia (Project CSD 2007-00010 Consolider-Ingenio in Molecular Nanoscience).

Appendix A. Supplementary materials

Supplementary data associated with this article can be found in the online version at doi:10.1016/j.jssc.2008.02.014.

References

[1] C. Sanchez, P. Gómez-Romero, Functional Hybrid Materials, Wiley VCH, Weinheim, 2004.
[2] E. Coronado, P. Day, Chem. Rev. 104 (2004) 5419–5448.
[3] E. Coronado, S. Curreli, C. Giménez-Saiz, C.J. Gómez-García, J. Mater. Chem. 15 (2005) 1429–1436.
[4] E. Coronado, S. Curreli, C. Giménez-Saiz, C.J. Gómez-García, Synth. Metals 154 (2005) 245–248.
[5] M. Kurmoo, A.W. Graham, P. Day, S.J. Coles, M.B. Hursthouse, J.L. Caulfield, J. Singleton, F.L. Pratt, W. Hayes, L. Ducasse, P.J. Guionneau, J. Am. Chem. Soc. 117 (1995) 12209–12217.
[6] E. Coronado, J.R. Galán-Mascarós, C.J. Gómez-García, V.N. Laukhin, Nature 408 (2000) 447–449.
[7] C. Bellitto, in: J.S. Miller, M. Drillon (Eds.), Magnetism: Molecules to Materials, vol. 2, Wiley-VCH, Weinheim, 2001, pp. 425–456 and references therein.
[8] C. Bellitto, F. Federici, S.A. Ibrahim, J. Chem. Soc. Chem. Commun. (1996) 759–760.
[9] C. Bellitto, F. Federici, S.A. Ibrahim, Chem. Mater. 10 (1998) 1076–1082.
[10] B. Bujoli, O. Pena, P. Palvadeau, J. LeBideau, C. Payen, J. Rouxel, Chem. Mater. 5 (1993) 583–587.
[11] A. Altomare, C. Bellitto, S.A. Ibrahim, M.R. Mahmoud, R.R. Rizzi, J. Chem. Soc. Dalton (2000) 3913–3919.
[12] C. Bellitto, F. Federici, A. Altomare, R.R. Rizzi, S.A. Ibrahim, Inorg. Chem. 39 (2000) 1803–1808.
[13] C. Bellitto, F. Federici, M. Colapietro, G. Portalone, D. Caschera, Inorg. Chem. 41 (2002) 709–714.
[14] P. Léone, P. Palvadeau, K. Boubekeur, A. Meerschaut, C. Bellitto, E.M. Bauer, G. Righini, P.J. Fabritchnyi, Solid State Chem. 178 (2005) 1125–1132.
[15] J.F. Penneau, B.J. Stallman, P.H. Kasai, L.L. Miller, Chem. Mater. 3 (1991) 791–796.
[16] T.M. Dietz, B.J. Stallman, W.S.V. Kwan, J.F. Penneau, J. Chem. Soc. Chem. Commun. (1990) 367–369.
[17] S. Brotchsztain, M.A. Rodriguez, G.F.J. Demets, M.J. Politi, J. Mater. Chem. 12 (2002) 1250–1255.
[18] C. Bellitto, E.M. Bauer, M. Colapietro, G. Portalone, G. Righini, Chem. Eur. J. 9 (2003) 1324–1331.
[19] B.N. Figgis, Introduction to Ligand Fields, Interscience, London, 1966, p. 221.
[20] M.M. Gómez-Alcántara, A. Cabeza, M. Martínez-Lara, A.A.G. Aranda, R. Suau, N. Bhunavesh, A. Clearfield, Inorg. Chem. 43 (2004) 5283–5293.
[21] A. Goni, J.L. Pizarro, L.M. Lezama, E.G. Barberis, M.I. Arriortua, T.J. Rojo, Mater. Chem. 6 (1996) 421–427.
[22] S. Brochsztain, M.J. Politi, Langmuir 15 (1999) 4486–4494.

[23] Y. Ofir, A. Zelichenok, S. Yitzchaik, J. Mater. Chem. 16 (2006) 2142–2149.
[24] R.L. Carlin, Magnetochemistry, Springer, Berlin, 1986, p. 149.
[25] M.E. Lines, J. Phys. Chem. Solids 31 (1970) 101–116.
[26] J.A. Bertrand, A.P. Ginsberg, R.I. Kaplan, C.E. Kirkwood, R.L. Martin, R.C. Sherwood, Inorg. Chem. 10 (1971) 240–246.
[27] J.M. Clemente-Juan, E. Coronado, J.R. Galán-Mascarós, C.J. Gómez-García, Inorg. Chem. 38 (1999) 55–63.
[28] C.A. Merrill, A.K. Cheetham, Inorg. Chem. 46 (2007) 278–284.
[29] J.A. Mydosh, Spin Glasses: An Experimental Introduction, Taylor & Francis, London, 1993.
[30] E. Coronado, J.R. Galán-Mascarós, C.J. Gómez-García, J.M. Martínez-Agudo, Inorg. Chem. 40 (2001) 113–120.
[31] E. Coronado, J.R. Galán-Mascarós, C.J. Gómez-García, J.M. Martínez-Agudo, Synth. Metals 122 (2001) 501–507.
[32] E. Coronado, J.R. Galán-Mascarós, C.J. Gómez-García, E. Martínez-Ferrero, M. Almeida, J. Waerenborgh, Eur. J. Inorg. Chem. (2005) 2064–2070.
[33] C. Deng-Ke, G. Song, Z. Li-Min, J. Solid State Chem. 177 (2004) 2311–2315.
[34] C. Bellitto, E.M. Bauer, P. Léone, G. Righini, C. Guillot-Deudon, A. Meerschaut, J. Solid State Chem. 179 (2006) 579–589.
[35] S.G. Carling, P. Day, D. Visser, R.K. Kremer, J. Solid State Chem. 106 (1993) 111–119.
[36] G.E. Fanucci, J. Krzysted, M.W. Meisel, L.C. Brunel, D.H. Talham, J. Am. Chem. Soc. 120 (1998) 5469–5479.